A Compact Single-Layer Substrate-Integrated Waveguide (SIW) Monopulse Slot Antenna Array

Feifei Cao, Deqiang Yang, Jin Pan, Dongdong Geng, and Hua Xiao

***Abstract*—In this study, a compact single-layer substrate-integrated waveguide (SIW) monopulse slot antenna array is designed. The antenna has a very simple structure and uses SIW-based cavity resonators, instead of a complex feeding network and monopulse comparator, to excite the slot array. The design decreases the size of the feeding network and monopulse comparator by applying cavity resonator principles to the monopulse slotted antenna array, resulting in an obvious improvement of the antenna aperture efficiency and structure complexity. This single-layer scheme, combined with a planar transmission line, is ideal for integration with planar circuits. A 16-element slot array prototype operating at 5.83 GHz is fabricated through a low-cost standard printed circuit board process to validate the design. The simulated and measured results are presented, and good agreement between them is obtained.**

***Index Terms*—Arrays, aperture efficiency, comparators, monopulse antennas.**

I. Introduction

MONOPULSE antennas are widely used in modern tracking applications due to their accurate direction-finding capability. The traditional monopulse antennas, such as parabolic antennas, slotted waveguide arrays, and lens antennas, are complicated, bulky, and costly to process. Efforts have been made to reduce the complexity and costs of monopulse antennas. Microstrip antenna arrays have been previously used to obtain a low profile and low cost in monopulse applications [1]–[4. However, the feeding network and monopulse comparator were distributed among the array elements, leading to spurious radiation and complexity in design. In recent years, with the development of a substrate-integrated waveguide (SIW) technology, many monopulse antennas based on the SIW technique have been reported. Compared with microstrip arrays, SIW-based antenna arrays have low loss and little spurious radiation. Several compact SIW monopulse antennas have multiple layers [5]–[7], with a slot array in the top layer, and a feeding network and monopulse comparator in the lower bottom layer. A compact cavity-backed monopulse antenna reported in [8] also applied a multilayer printed circuit board (PCB) and an SMA feed pointing to the backside of the cavity. In [9], the SIW-based monopulse antenna arrays with filtering features also had multiple layers. Compared with multilayer monopulse antennas, single-layer antennas are less complicated and easier to integrate into a planar PCB. In [10] and [11], SIW-based single-layer monopulse antenna arrays are reported, with all the components of the feeding network and monopulse comparator, such as the power divider, 3 dB coupler, and phase shifter, creatively fabricated on a single-layer PCB. These works further reduced the complexity of the antenna structure. In the conclusion of [10], Liu et al. mentioned that the structure was significantly larger than the radiating aperture; thus, the corresponding aperture efficiency was small, which was the trade off for the compact size. The same is true in [10]–[12], in which a large portion of the antenna surface is occupied by the feeding network and monopulse comparator. Because the area of the feeding network and monopulse comparator is larger than the radiation aperture, the antenna aperture efficiency is significantly degraded.

In this study, we propose an alternative solution to obtain a monopulse antenna array on a single-layer PCB. SIW cavity resonators are used to excite an SIW slot array. No complex monopulse comparator or feeding network is needed. Furthermore, with a high-order mode in the SIW cavities [13], the feeding network size is further decreased. The antenna is compact, low-cost, low-profile, and single-layer, and both feeding ports are planar transmission lines on the same surface of the antenna array, which is ideal for integration into a planar PCB. Most of all, the proposed solution improves the antenna aperture efficiency and shows a compact way of implementing monopulse performance.

II. Antenna Configuration and Working Principles

The proposed monopulse antenna consists of four SIW cavities and two feeding ports. All structures are integrated into a single-layer PCB. Fig. 1 shows the configuration of the antenna prototype. Cavities 1 and 2 are used to achieve the functions of the monopulse comparator and feeding network. This structure design considerably decreases the area occupied by the comparator and feeding network on a single-layer PCB. There are 16 slots on cavities 3 and 4 that are used for radiation. This can be regarded as a combination of four 4×1 SIW-based waveguide longitudinal slot antenna subarrays. Moreover, all the cavities are connected by some openings. Port 1 is the difference

Manuscript received July 28, 2017; accepted August 20, 2017. Date of publication August 25, 2017; date of current version October 2, 2017. *(Corresponding author: Feifei Cao.)*

F. Cao, D. Geng, and H. Xiao are with the University of Electronic Science and Technology of China, Chengdu 610054, China (e-mail: 147298367@qq.com; 1198216866@qq.com; 408815597@qq.com).

D. Yang and J. Pan are with the Department of Microwave Engineering, School of Electronic Engineering, University of Electronic Science and Technology of China, Chengdu 610054, China (e-mail: dqyang@uestc.edu.cn; panjin@uestc.edu.cn).

Color versions of one or more of the figures in this letter are available online at http://ieeexplore.ieee.org.

Digital Object Identifier 10.1109/LAWP.2017.2744668

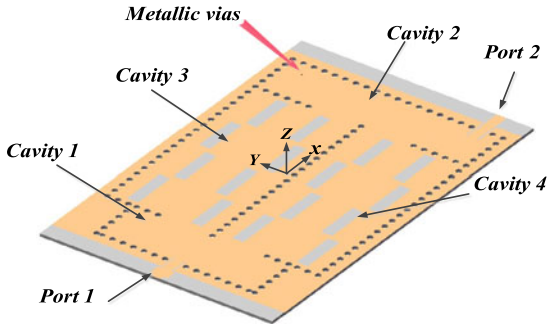

Fig. 1. Antenna configuration.

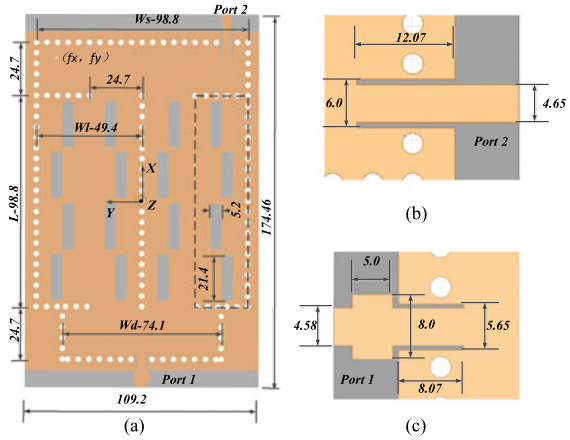

Fig. 2. Antenna dimensions (in mm): (a) antenna profile, (b) port 2, and (c) port 1.

beam feed. Port 2 is the sum beam feed. These feed ports are 50 Ω microstrip lines. Fig. 2(b) and (c) shows the details of the two ports. Metallic vias are introduced in cavity 2 for frequency tuning.

Fig. 2 shows the dimensions of the proposed antenna prototype. The substrate is 1.5 mm thick, with a dielectric constant of 2.2. The origin of the coordinate is at the center of the antenna. The metallic vias are at $f_x = 66.75$ mm, $f_y = 40.65$ mm. The antenna operates at 5.83 GHz. W_s and L are 4 half-waveguides in length, W_d is 3 half-waveguides in length, and W_l is 2 half-waveguides in length. The four cavities can be regarded as one unit. Due to their boundary condition, these cavities can have many eigenmodes, two of which are obvious and ideal for achieving a monopulse beam pattern. Fig. 3 shows the expected magnitude distribution of the two eigenmodes, which are standing-wave patterns. The plus and minus signs indicate the field orientation, and the dashed line indicates the openings by which the cavities are joined together. Energy is coupled through the dashed line between cavities. Fig. 3(a) shows the expected oscillating mode inside the antenna when cavity 2 is excited by port 2. The fields that are coupled in cavities 3 and 4 are opposite in phase. Under this condition, the field coupled in cavity 1 is either canceled or has a nodal point at the position of port 1. Thus, ports 1 and 2 are isolated under this mode. Fig. 3(b) shows the expected oscillating mode inside the antenna when cavity 1 is excited by port 1.

The field that is coupled in cavities 3 and 4 is in phase. Under this condition, the field coupled in cavity 2 will not cause

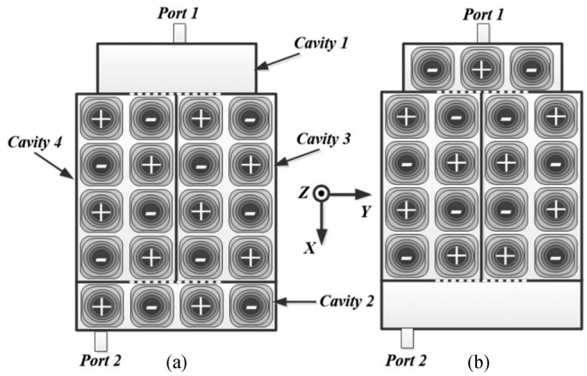

Fig. 3. Predicted eigenmodes inside the antenna cavity: the field distribution (a) when port 2 is excited and (b) when port 1 is excited.

effective resonance. Port 2 can be either at the left or at the right side of cavity 2; these positions can minimize field coupling from cavities 3 and 4.

The standing-wave patterns inside the antenna cavities, as shown in Fig. 3, lead us to cut the radiating slots on the top surface of cavities 3 and 4. The slots are spaced at half-waveguide wavelength, which introduces a 180° change of phase, and are positioned alternately on the opposite sides of the standing wave peak centerlines to add another 180°-phase [13]. When port 1 is excited, the slots in cavities 4 and 3 radiate fields in the opposite phase; thus, a difference in the radiation patterns is expected. When port 2 is excited, the slots in cavities 4 and 3 radiate fields in phase; thus, a sum radiation pattern is expected.

III. Simulated and Measured Results

To verify the existence of the two predicted eigenmodes in Fig. 3, we simulated the cavity field distribution without radiating slots. Fig. 4 shows the simulated field distribution inside the antenna cavity. Fig. 4(a) presents the field distribution when port 2 is excited, and Fig. 4(b) shows the field distribution when port 1 is excited. The field distribution is consistent with the prediction. The openings between the cavities caused a slight deformation of the field distribution compared with Fig. 3, but had only a limited effect on the antenna radiation pattern. Also, when port 1 is excited, there is coupling between cavities 3 and 4. However, this is not an issue in such a situation because reasonably different patterns are obtained even in the presence of the coupling.

Regarding the antenna resonant frequency, it should be noted that the field patterns in Fig. 4(a) and (b) correspond to different eigenmodes. This means that although the sum and difference beam patterns share the same radiation cavities, they can still resonate at different frequencies. In the initial model of the proposed antenna, in which no metallic vias are introduced, the central frequency of port 1 is 80 MHz offset from port 2, as determined by HFSS software simulation. Metallic vias (with a radius equal to 0.45 mm), as shown in Fig. 1, are introduced to eliminate the frequency offset. Moving the vias slightly toward $-y$ will "squeeze" the standing wave distribution in cavity 2 into a smaller room; thus, the resonant frequency of the sum pattern will increase a little bit. Contrarily, moving the vias along the $+y$-axis will "extend" the room to fit the standing waves; thus,

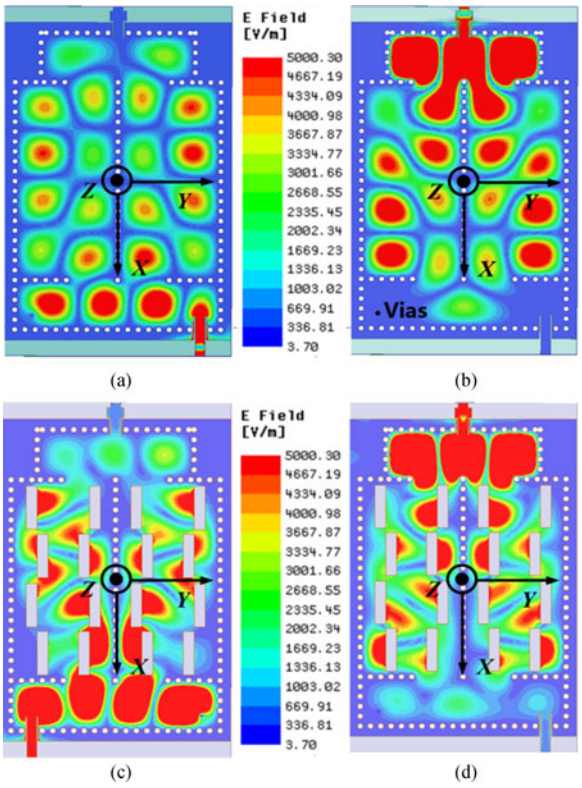

Fig. 4. Simulated field distribution inside the antenna cavity: the field distribution (a) when port 2 is excited, (b) when port 1 is excited, (c) when port 2 is excited in the presence of slotted arrays, and (d) when port 1 is excited in the presence of slotted arrays.

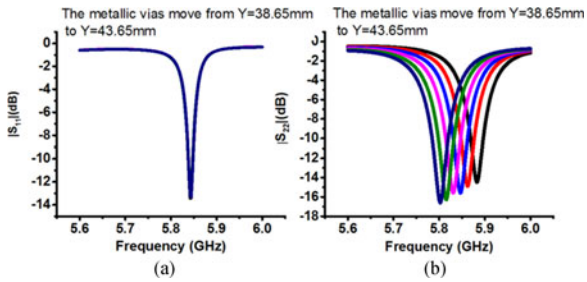

Fig. 5. Frequency tuning by moving the metallic vias: (a) difference port $|S_{11}|$ and (b) sum port $|S_{22}|$.

the central frequency will decrease. Moreover, this fine-tuning affects only the sum pattern frequency and not the difference pattern. As shown in Fig. 4(b), when the difference pattern is excited, there is no field distribution around the point where the metallic vias are; thus, moving the metallic vias slightly will not disturb the field distribution of the difference pattern at all. Fig. 5 shows the simulated frequency tuning obtained by moving the vias from $f_x = 66.75$ mm, $f_y = 38.65$ mm to $f_x = 66.75$ mm, $f_y = 43.65$ mm at a step of 1 mm. As shown in Fig. 5(a), the resonant frequency of $|S_{11}|$ does not change at all, and all the curves are overlapped. However, the resonant frequency of $|S_{22}|$, as shown in Fig. 5(b), decreases from 5.88 to 5.80 GHz with the increase in the y position.

The proposed antenna is fabricated by using a low-cost standard PCB. Measurements of the return loss are carried out by applying an Agilent N5230A network analyzer; the gain and

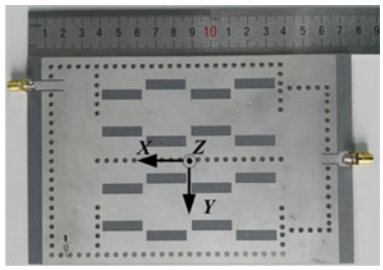

Fig. 6. Photograph of the prototype with a tuning hole and SMA connectors.

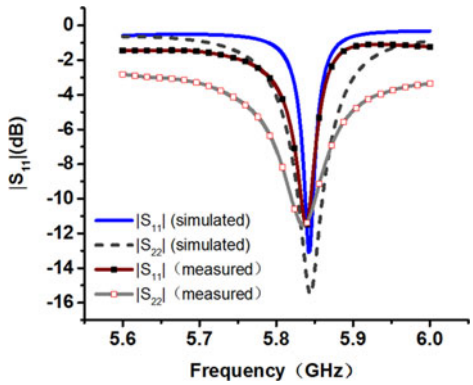

Fig. 7. Simulated and the measured $|S_{11}|$ and $|S_{22}|$ parameters.

radiation pattern are measured on a far-field antenna measurement system. Fig. 6 shows a photograph of the fabricated prototype with SMA connectors, and a hole is manually drilled to verify whether the frequency tuning method is identical with the simulated prediction. As shown in Fig. 7, the measured resonant frequency of ports 1 and 2 is successfully overlapped by applying this tuning method.

Fig. 7 shows the measured and the simulated return losses, which are in good agreement. A small discrepancy is observed, which may be attributed to fabrication tolerance, permittivity fluctuation, and slight warping of the substrate. The measured central frequency is 5.83 GHz. The simulated central frequency is 5.84 GHz.

Fig. 8(a) and (b) shows the simulated and the measured difference and sum patterns with the cross-polarization patterns. The simulated cross polarization is -26.9 dB compared with the sum max. The measured cross polarization is -17 dB. The difference between the simulated and the measured cross polarization could be caused by antenna processing error and antenna measurement error. The simulated gain of the sum pattern is 14.22 dBi, and the null depth is 28.6 dB. The measured gain of the sum pattern is 12.9 dBi, and the null depth is 40 dB. Fig. 8(c) and (d) shows the comparison between the simulated and the measured yz-plane patterns. Fig. 8(e) shows the comparison of the xz-plane patterns. There is good agreement between the simulated and the measured patterns.

Aperture efficiency $\eta = \frac{\lambda^2 G}{4\pi A}$. G is the antenna gain. A is the antenna aperture area. λ is the wavelength.

A comparison is presented in Table I, in which the proportionality coefficient is defined as the approximate proportion of the feeding network and monopulse comparator area to the radiating aperture area. In a single-layer microstrip array [1],

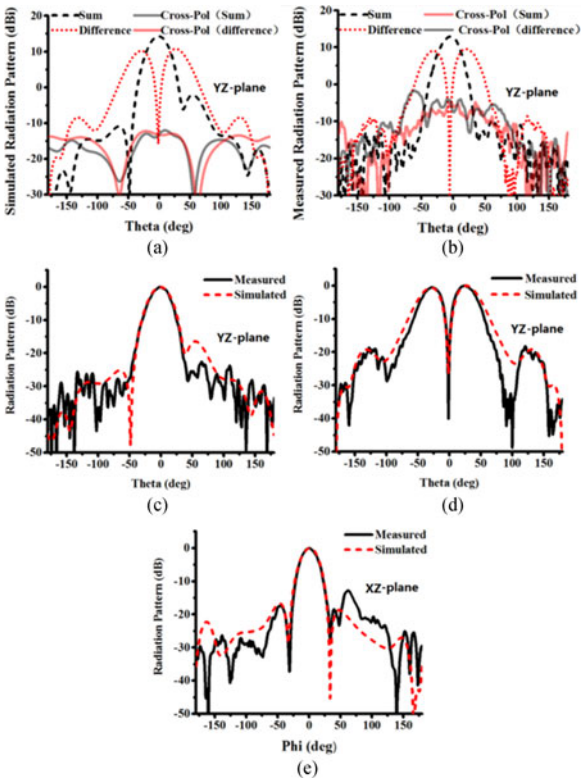

Fig. 8. Simulated and the measured radiation patterns: (a) the simulated sum and difference patterns with the cross-polarization patterns in the *yz* plane, (b) the measured sum and difference patterns with the cross-polarization patterns in the *yz* plane, (c) comparison of the simulated and measured sum patterns in the *yz* plane, (d) comparison of the simulated and measured difference patterns in the *yz* plane, and (e) comparison of the simulated and measured patterns in the *xz* plane.

TABLE I
COMPARISON OF SINGLE-LAYER MONOPULSE ANTENNA ARRAY

Antenna	f_0 (GHz)	Aperture size (wavelength)	Proportionality Coefficient	Gain (dBi)	Aperture Efficiency
[1]	14.25	13.3 ∗ 12.35	0	24.5	14%
[4]	31.5	14.49 ∗ 10.39	2	18.74	4%
[12]	94	40.73 ∗ 39.16	2	25.75	2%
[14]	10	4.4 ∗ 1.02	2	9.6	16%
Proposed antenna	5.83	2.12 ∗ 3.39	0.5	12.9	21%

the feeding network and monopulse comparator are embedded into the gaps between patch elements. This does not increase the antenna aperture size. However, the microstrip network is lossy and leads to spurious radiation. In single-layer SIW arrays [4], [12], [14], there is no spurious radiation from the network and lower loss. However, the size of the area of the feeding network and monopulse comparator is twice that of the radiating aperture size because the power divider, phase shifter, and 3 dB directional couplers occupy a large portion of the antenna aperture, resulting in a proportionality coefficient as large as 2. In this work, the application of cavity resonator principles to monopulse slotted array antennas and the use of a cavity resonator instead of a network decreased the size of the antenna aperture; thus, the proportionality coefficient of the proposed antenna is only 0.5, and it shows a compact way of implementing monopulse performance.

IV. CONCLUSION

In this study, a compact single-layer SIW monopulse antenna array is proposed and fabricated to show the application of cavity resonator principles to monopulse slotted array antennas. The use of a cavity resonator instead of a feeding network and monopulse comparator considerably decreased the size of the antenna aperture on a single-layer PCB. The feeding network area is only half the size of the antenna aperture, and it shows a compact way of implementing monopulse performance. Good agreement between the simulation and the measurement results is observed. The proposed antenna array is thus a good candidate for use in low-cost, simple-structure, compact-size tracking system applications. The idea of adopting cavity resonator principles to monopulse slotted array antennas can be applied to larger monopulse antenna arrays to reduce their structure complexity and network size.

REFERENCES

[1] H. Wang, D.-G. Fang, and X. G. Chen, "A compact single layer monopulse microstrip antenna array," *IEEE Trans. Antennas Propag.*, vol. 54, no. 2, pp. 503–509, Feb. 2006.
[2] B. J. Andrews, T. S. Moore, and A. Y. Niazi, "Millimeter wave microstrip antenna for dual polar and monopulse applications," in *Proc. 3rd Int. Conf. Antennas Propag.*, Apr. 1983, pp. 12–15.
[3] C. M. Jackson, "Low cost K-band microstrip patch monopulse antenna," *Microw. J.*, vol. 30, no. 7, pp. 125–126, 1987.
[4] S. G. Kim and K. Chang, "Low-cost monopulse antenna using bi-direction ally-fed microstrip patch array," *Electron. Lett.*, vol. 39, no. 20, pp. 1428–1429, 2003.
[5] T. Li and W. Dou, "A monopulse slot array antenna based on dual-layer substrate integrated waveguide (SIW)," in *Proc. 2016 IEEE 5th Asia-Pac. Conf. Antennas Propag.*, 2016, pp. 373–374.
[6] J. L. Masa-Campos, M. Sierra-Perez, J. L. Fernandez-Jambrina, and P. Rodriguez-Fernandez, "New circularly polarized slot radiator for substrate integrated waveguide (SIW) planar array," in *Proc. 5th Eur. Conf. Antennas Propag.*, 2011, pp. 816–820.
[7] K. Tekkouk, M. Ettorre, and R. Sauleau, "SIW pillbox antenna for monopulse radar applications," *IEEE Trans. Antennas Propag.*, vol. 63, no. 9, pp. 3918–3927, Sep. 2015.
[8] H. Gharibi and F. Hodjatkashani, "Design of a compact high-efficiency circularly polarized monopulse cavity-backed substrate integrated waveguide antenna," *IEEE Trans. Antennas Propag.*, vol. 63, no. 9, pp. 4250–4256, Sep. 2015.
[9] Z. H. Fan, Z. He, S. Luo, and Y. Guo, "A millimeter-wave filtering monopulse antenna array based on substrate integrated waveguide technology," *IEEE Trans. Antennas Propag.*, vol. 64, no. 1, pp. 316–321, Jan. 2016.
[10] B. Liu *et al.*, "Substrate integrated waveguide (SIW) monopulse slot antenna array," *IEEE Trans. Antennas Propag.*, vol. 57, no. 1, pp. 275–279, Jan. 2009.
[11] Y. J. Cheng, W. H., and K. Wu, "94 GHz substrate integrated monopulse antenna array," *IEEE Trans. Antennas Propag.*, vol. 60, no. 1, pp. 121–129, Jan. 2012.
[12] Z. C. Hao, H. H. Wang, and W. Hong, "A novel planar reconfigurable monopulse antenna for indoor smart wireless access points' application," *IEEE Trans. Antennas Propag*, vol. 64, no. 4, pp. 1250–1261, Apr. 2016
[13] H. Wang, F. Yang, R. Long, L. Zhou, and F. Yan, "Single-fed low-profile high-gain circularly polarized slotted cavity antenna using a high-order mode," *IEEE Antennas Wireless Propag. Lett.* vol. 15, pp. 110–113, 2016.
[14] J. F. Xu, Z. N. Chen, X. M. Qing, and W. Hong, "A single-layer SIW Slot array antenna with TE20 Mode" in *Proc. Asia-Pac. Microw. Conf.*, 2011, pp. 1330–1333.